

CONFERENCES AND SYMPOSIA PACS number: 01.10.Fv

Joint scientific session of the Physical Sciences Division of the Russian Academy of Sciences and the Joint Physical Society of the Russian Federation 'Backward waves' (25 January 2006)

The Physical Sciences Division of the Russian Academy of Sciences and the Joint Physical Society of the Russian Federation held a joint session on backward waves in the conference room of the Lebedev Physics Institute, RAS, on 25 January 2006. The following reports were presented at the session:

1. **Veselago V G** (Moscow Institute for Physics and Technology, Prokhorov Institute of General Physics, RAS). "Negative refraction and backward waves";

2. **Vashkovsky A V, Lock E H** (Institute of Radio-Electronics, Fryazino, Moscow region). "Forward and backward noncollinear waves in magnetic films";

3. **Silin R A** (FGUP 'NPP Istok'). "Electromagnetic waves in artificial periodic structures."

Below are brief summaries of the last two contributions. The key points of Veselago's talk can be found in *Usp. Fiz. Nauk* **172** 1215 (2002) [*Phys. Usp.* **45** 1097 (2002)])

PACS numbers: **41.20.–q**, 78.20.Ci, **78.66.–w**
DOI: 10.1070/PU2006v049n05ABEH006035

Forward and backward noncollinear waves in magnetic films

A V Vashkovsky, E H Lock

Thin layers of magnetically ordered media (ferrites, for example) allow the excitation and low-loss propagation of electromagnetic waves for which, at ultrahigh (microwave) frequencies, the wave vector k has a value between 10 and 10^4 cm^{-1}, i.e., much larger than for the vacuum: $k \gg k_0 \equiv \omega/c \sim 1\,\text{cm}^{-1}$. These waves, known as dipole spin waves or magnetostatic waves (MSWs), have a remarkably low group velocity v_g, around 1 – 1000 km c^{-1}, and the angle between their wave vector **k** and the group velocity vector $\mathbf{v}_g$ may take any value between 0 and 180°. This feature is of particular interest because it enables both forward and backward waves to be easily excited in an experiment.

Uspekhi Fizicheskikh Nauk **176** (5) 557 – 565 (2006)
Translated by E G Strel'chenko; edited by A M Semikhatov

We consider an infinitely extended, parallel-plane ferrite plate (or film) 2, of thickness s, sandwiched between vacuum half-spaces 1 and 3 (we use the indices $j = 1, 2, 3$ to label the field and other parameters in the respective media). We choose the Cartesian coordinate system such that the x axis is perpendicular to the plane of the plate and the tangential uniform magnetic field is parallel to the z axis. The plate is supposed to be magnetized to saturation and is characterized by a relative dielectric constant ε_2 and a magnetic permeability tensor $\overleftrightarrow{\mu_2}$ of the form

$$\overleftrightarrow{\mu_2} = \begin{vmatrix} \mu & \mathrm{i}\nu & 0 \\ -\mathrm{i}\nu & \mu & 0 \\ 0 & 0 & \mu_z \end{vmatrix}, \tag{1}$$

where

$$\mu = 1 + \frac{\omega_M \omega_H}{\omega_H^2 - \omega^2}\,, \tag{2}$$

$$\nu = \frac{\omega_M \omega}{\omega_H^2 - \omega^2}\,, \tag{3}$$

$\omega_H = \gamma H_0$, $\omega_M = 4\pi\gamma M_0$, $\omega = 2\pi f$, γ is the gyromagnetic constant, $4\pi M_0$ is the saturation magnetization of the ferrite, and f is the electromagnetic oscillation frequency. The electromagnetic field in the plate satisfies the Maxwell equations. Using the method of complex amplitudes (with $\exp(\mathrm{i}\omega t)$ in the inverse Fourier transform), we can write them as

$$\begin{aligned} &\mathrm{rot}\,\mathbf{H}_j = \mathrm{i}\,\frac{\omega}{c}\,\varepsilon_j \mathbf{E}_j\,, \\ &\mathrm{rot}\,\mathbf{E}_j = -\mathrm{i}\,\frac{\omega}{c}\,\mu_j \mathbf{H}_j\,, \\ &\mathrm{div}\,(\varepsilon_j \mathbf{E}_j) = 0\,, \\ &\mathrm{div}\,(\mu_j \mathbf{H}_j) = 0\,, \end{aligned} \tag{4}$$

where $\mathbf{H}_j$ and $\mathbf{E}_j$ are complex amplitudes of the electric and magnetic field strengths, ε_j and μ_j are the parameters of the medium ($j = 1-3$), and c is the speed of light in the vacuum.

With the y axis (perpendicular to $\mathbf{H}_0$) taken as the direction of the electromagnetic wave in the film plane and the problem assumed to be uniform along the z axis, i.e., $\partial\mathbf{H}_j/\partial z = \partial\mathbf{E}_j/\partial z \equiv 0$, system (4) for the fields within the plate

decouples into two independent subsystems

$$\begin{cases} \dfrac{\partial H_{2y}}{\partial x} - \dfrac{\partial H_{2x}}{\partial y} = \mathrm{i}\,\dfrac{\omega}{c}\,\varepsilon_2 E_{2z}\,, \\ \dfrac{\partial E_{2z}}{\partial y} = -\mathrm{i}\,\dfrac{\omega}{c}\,(\mu H_{2x} + \mathrm{i}\nu H_{2y})\,, \\ \dfrac{\partial E_{2z}}{\partial x} = \mathrm{i}\,\dfrac{\omega}{c}\,(-\mathrm{i}\nu H_{2x} + \mu H_{2y})\,, \end{cases} \qquad (5)$$

$$\begin{cases} \dfrac{\partial H_{2z}}{\partial y} = \mathrm{i}\,\dfrac{\omega}{c}\,\varepsilon_2 E_{2x}\,, \\ \dfrac{\partial H_{2z}}{\partial x} = -\mathrm{i}\,\dfrac{\omega}{c}\,\varepsilon_2 E_{2y}\,, \\ \dfrac{\partial E_{2y}}{\partial x} - \dfrac{\partial E_{2x}}{\partial y} = -\mathrm{i}\,\dfrac{\omega}{c}\,\mu_z H_{2z}\,, \end{cases}$$

where E_{2x}, E_{2y}, E_{2z}, H_{2x}, H_{2y}, and H_{2z} are the projections of the vectors $\mathbf{E}_2$ and $\mathbf{H}_2$ on the corresponding axes. The first subsystem describes a TE wave with components E_z, H_x, H_y, and the second describes a TH wave with components E_x, E_y, H_z. The TH wave interacts with the material of the film through the tensor component $\overleftrightarrow{\mu_2}$, which is $\mu_z = 1$, and in fact 'perceives' the ferrite plate as an ordinary nonmagnetic insulator. The first equation of system (5) — the one for the TE wave — involves the components of the tensor $\overleftrightarrow{\mu_2}$, which can be varied from $-\infty$ to $+\infty$ by varying the frequency or magnitude of the field H_0.

System (5) for the TE wave is solved for the E_{2z} component and is reduced to the Helmholtz equation

$$\frac{\partial^2 E_{2z}}{\partial x^2} + \frac{\partial^2 E_{2z}}{\partial y^2} + k_0^2 \varepsilon_2 \mu_\perp E_{2z} = 0 \qquad (6)$$

with $k_0 = \omega/c$ and $\mu_\perp = (\mu^2 - \nu^2)/\mu$. The solution for E_{2z} can be written as

$$E_{2z} = \exp(-\mathrm{i}k_y y)\left[A\exp(k_{2x}x) + B\exp(-k_{2x}x)\right], \qquad (7)$$

where A and B are arbitrary constants and k_{2x} and k_y are the wave vector projections related by

$$k_y^2 - k_{2x}^2 = q_2^2 = k_0^2\,\varepsilon_2\,\mu_\perp\,. \qquad (8)$$

Satisfying the continuity of the tangential components $\mathbf{E}$ and $\mathbf{H}$ at the plate interfaces yields the dispersion relation

$$\tanh(k_{2x}\,s) = -\frac{2\mu\sqrt{1-(k_0/k_y)^2}\,\sqrt{1-\varepsilon_2\mu_\perp(k_0/k_y)^2}}{1+\mu^2-\nu^2-(\,\mu\varepsilon_2+\mu^2-\nu^2)(k_0/k_y)^2} \qquad (9)$$

between the frequency ω, the wave vector k, the layer thickness s, and the material parameters.

Based on (9), we calculate the dispersion relation $f(k_y)$ for the TE wave of interest for parameters typically used in experiments: $H_0 = 300$ Oe, $4\pi M_0 = 1750$ G, $\varepsilon_2 = 15$, and $s = 10$ μm (curve *1* in Fig. 1). As seen from Fig. 1, the phase velocity of the TE wave is reduced by a factor of 10 to 1000 from its vacuum value. With this slowdown, the time-derivative terms in the Maxwell equations can obviously be ignored, which leads to the magnetostatic equations

$$\mathrm{rot}\,\mathbf{H}_j = 0\,, \qquad (10)$$

$$\mathrm{div}(\mu_j\,\mathbf{H}_j) = 0\,. \qquad (11)$$

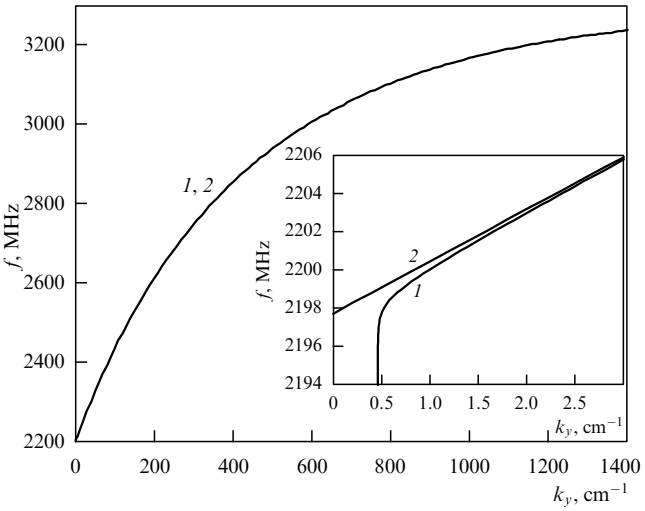

Figure 1. Dispersion relations for a magnetostatic wave propagating perpendicular to $\mathbf{H}_0$: *1*, from the Maxwell equations; *2*, in the magnetostatic approximation.

We next introduce the magnetostatic potential defined by $\mathbf{H}_j = \mathrm{grad}\,\Psi$ and use Eqns (10) and (11) to obtain equations for Ψ inside and outside the plate. Using the well-known boundary conditions (the normal magnetic flux and potential continuity at each ferrite – vacuum boundary) yields a system of equations that gives the following dispersion equation for the y-propagating wave:

$$\tanh\,(k_y s) = -\frac{2\mu}{1+\mu^2-\nu^2}\,. \qquad (12)$$

In Fig. 1, the dependence $f(k_y)$ calculated from Eqn (12) is indistinguishable from the exact curve obtained from Eqn (9). The only region where the curves can be distinguished — that of small values for $k_y \sim k_0$ — is shown in the inset of the figure. As we see, even for the wave numbers 2 – 3 cm^{-1}, the difference in frequency is given by several parts of a megahertz. Comparing Eqns (12) and (9), we conclude similarly that assuming $(k_0/k_y)^2 \ll 1$ and neglecting terms containing $(k_0/k_y)^2$ transforms Eqn (9) into Eqn (12).

To summarize, if we sacrifice a small initial interval of k_y and the corresponding region of f — i.e., if we do not use Eqn (12) when describing the TE wave for $k \sim k_0$ — then it is quite legitimate to use the magnetostatic approximation to describe this wave. This means losing the expression for the field E_z, but it is not necessary in most of the problems. The boundary equations of magnetostatics — the potential and normal magnetic flux continuity — are equivalent to the continuity of the tangential components of $\mathbf{E}$ and $\mathbf{H}$. The solution we obtain is simpler in form and makes it easy to describe wave propagation at an arbitrary angle to the y axis. For an arbitrary wave propagation direction, the dispersion is described by the transcendental equation

$$\tanh\,(k_{2x}s) = -\frac{2\mu k_{1x}k_{2x}}{k_{1x}^2 + \mu^2 k_{2x}^2 - \nu^2 k_y^2}\,, \qquad (13)$$

where the x-components of the wave vector in the plate and vacuum are given by

$$k_{2x} = \sqrt{-k_y^2 - \frac{k_z^2}{\mu}}\,,$$

$$k_{1x} = \sqrt{k_y^2 + k_z^2}\,. \qquad (14)$$

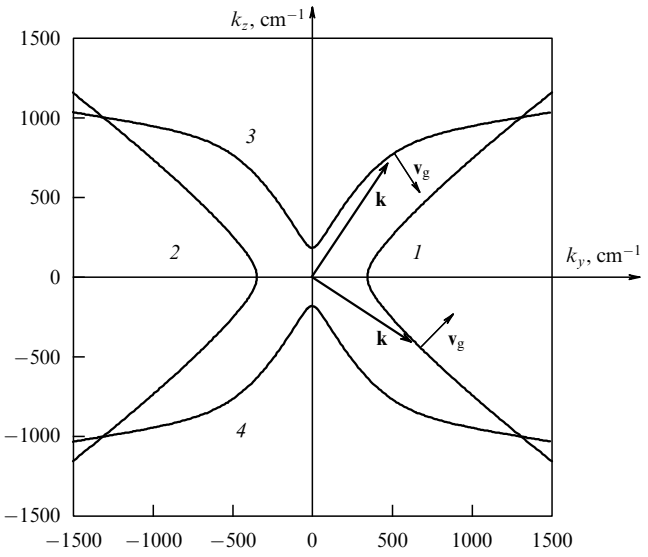

Figure 2. Isofrequency curves for $f = 2800$ MHz, $4\pi M_0 = 1750$ G, and $s = 10$ μm: curves *1*, *2* for a forward MSW at $H_0 = 300$ Oe; curves *3*, *4* for a backward MSW at $H_0 = 480$ Oe.

Solutions of this equation for a fixed frequency — the so-called isofrequency curves — are shown in Fig. 2 for two magnetization values. It can be seen that the vector **k** deviates from the z axis or the y axis as its absolute magnitude increases — implying that the static approximation is not violated.

Before proceeding further, we recall that the direction of the group velocity vector $\mathbf{v}_g$ is determined by the normal to the isofrequency curve. We also clarify the terms to be used in what follows. The term 'forward' refers to a wave for which the scalar product $\mathbf{k}\mathbf{v}_g > 0$, and the term 'backward' to a wave for which $\mathbf{k}\mathbf{v}_g < 0$. This definition applies irrespective of the medium in which the wave propagates (i.e., of whether it is isotropic or anisotropic) and is more general than the one usually found in textbooks, dictionaries, and encyclopedias, where only collinearly propagating waves (with **k** and $\mathbf{v}_g$ parallel to each another) are considered.

The group velocity vectors $\mathbf{v}_g$ for two arbitrarily chosen vectors **k** are shown in Fig. 2, where it is seen that for $H_0 = 300$ Oe (curves *1* and *2*), Eqn (14) describes a *forward wave*, with $\mathbf{k}\mathbf{v}_g > 0$ and $|\partial\omega/\partial\mathbf{k}| > 0$; for $H_0 = 480$ Oe (curves *3* and *4*), it describes a *backward wave*, with $\mathbf{k}\mathbf{v}_g < 0$ and $|\partial\omega/\partial\mathbf{k}| < 0$. It is relevant to note that the vectors **k** and $\mathbf{v}_g$ of the forward wave are collinear only when **k** is parallel to the y axis, and those of the backward wave only when **k** is parallel to the z axis. The directions along which the vectors **k** and $\mathbf{v}_g$ are collinear and the isofrequency curves are symmetric are the optical axes of the medium. A wave propagating along an optical axis is referred to as collinear (it may be either forward or backward), and a wave propagating at the right angle to an optical axis as noncollinear (it can be either type as well).

The two branches of the isofrequency dependences for the forward (curves *1* and *2*) and backward (curves *3* and *4*) waves are absolutely identical and describe wave propagation in opposite directions. The separation between the branches of the isofrequency curve depends on the magnetization field, for both the forward and the backward waves. That is, the branches can come closer together or move farther apart as the magnet field is varied. For the forward wave, the two branches, *1* and *2*, of the isofrequency curve not only look like, but in fact are very closely approximated by hyperbolas. This suggests the following point. If we bring the branches of the isofrequency curves closer together and recall the TM wave that we have neglected, we find a situation similar to what is well known to occur in a birefringent uniaxial crystal. For the TM wave, the ferrite film is isotropic, whereas the isofrequency curve is (or looks very much like) a circle with a radius about 1 cm^{-1}. Thus, the plane of the ferrite plate supports two waves with different refraction indices, one of them being dependent on and the other independent of the wave propagation direction. We therefore have a model of a birefringent uniaxial crystal, but with a very interesting and important twist: the index of refraction of this unusual wave is described not by an ellipse but by a *hyperbola*!

Below, we discuss some characteristics of forward and backward TE waves or those of MSWs propagating at an arbitrary angle to an optical axis; the TM wave is not practically excited in thin ferrite plates and is not mentioned in the discussion below, all the more so because it is quite trivial in propagation, reflection, and refraction terms.

In Fig. 3, the orientation of the group velocity vector (the angle ψ between the vector $\mathbf{v}_g$ and the y axis) is shown as a function of the orientation of the wave vector (the angle φ between **k** and the y axis) for the forward and backward waves (here and below, the angles ψ and φ are measured positively in the counterclockwise direction). It is seen that the dependence $\psi(\varphi)$ is single-valued for the forward wave and is not single-valued for the backward wave. Therefore, it may happen as the backward wave propagates that two (or occasionally even three) beams differing in the direction and magnitude of the wave vector (or, in other words, in the wavelength and wave front orientation) propagate in the same direction. For example, for $\psi = -60°$, two beams with different orientations of wave fronts ($\varphi = 54°$ and $\varphi = 85°$) may propagate.

Knowing the basic characteristic of an MSW beam, the dependence $\psi(\varphi)$, it is easy to consider the reflection and refraction of the forward and backward noncollinear waves. We first take a general look at reflection. Let the beam be incident on a flat mirror (straight-line edge of a ferrite film).

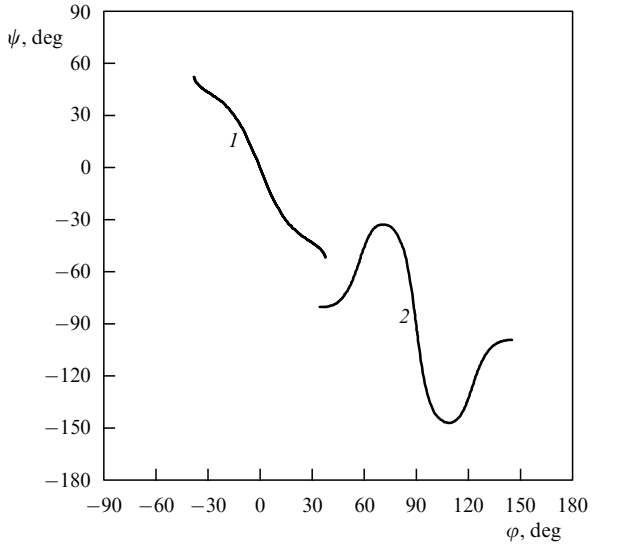

Figure 3. Direction of the backward wave group velocity (the angle ψ) versus the wave vector orientation (the angle φ) for $f = 2800$ MHz, $4\pi M_0 = 1750$ G, and $s = 10$ μm: curve *1*, forward MSW for $H_0 = 300$ Oe (corresponding to curve *1* in Fig. 2); curve *2*, backward MSW for $H_0 = 480$ Oe (corresponding to curve *3* in Fig. 2).

Depending on the angle between the optical axis of the medium and the mirror plane normal, several types of reflection are recognized, differing in the relative geometry of the incident and reflected beams. For the optical axis coinciding with the mirror plane normal, the properties of the medium are symmetric with respect to the normal, and reflection obeys Euclid's law: the angle of incidence is equal to the angle of reflection. When the optical axis deviates from the normal, the wave properties of the medium turn out to be asymmetric with respect to the normal, leading to a difference between the incidence and reflection angles. Further deviation from the optical axis gives rise to reversed (or negative) reflection, the most unusual situation occurring when an obliquely incident beam is reflected in the direction opposite to the incident direction. At large deviations, a forward noncollinear wave incident on the mirror in a broad sector of 40 to 45° has its beams reflected to a narrow sector of the order of 2–3°, i.e., a *flat* mirror focuses the reflected beams into a narrow beam. As the optical axis deviates still further, a situation occurs in which the mirror plane normal coincides with the asymptote to the isofrequency curve (which is a hyperbola for the forward MSW); in this case, a beam never produces a reflection, whatever its angle of incidence. The explanation is that the second branch of the isofrequency hyperbola lies on the other side of the asymptote, and there exist no beams that satisfy the boundary conditions at the surface of the mirror. So much for a general outline of how a noncollinear wave is reflected. All the above situations have been observed experimentally [2–4]. Some time after our first experiments [2], a theoretical study of a similar situation was made [5].

Another important point in studying wave reflection is that in contrast to isotropic media, where it does not matter whether the mirror or the exciting antenna is rotated to change the wave incidence angle to the flat mirror, these two approaches lead to totally different results in an anisotropic medium because the mirror or antenna also change their orientation relative to the optical axis when rotated. Clearly, when the mirror is turned, the *parameters of the incident wave* (the wavelength λ_i, the wave vector $\mathbf{k}_i$, the group velocity $\mathbf{v}_{gi}$, and their associated angles φ_i and ψ_i) *remain constant*, whereas when the antenna is turned, the *parameters of the incident wave are different for each new angle of incidence* (because the vectors $\mathbf{k}_i$ and $\mathbf{v}_{gi}$ change orientation relative to the optical axis). We note that the wave vector k_r of the reflected beam may differ considerably from k_i.

We first consider what happens when a *forward collinear wave* is incident on a flat mirror of varying orientation relative to the optical axis [6]. Figure 4 shows the calculated angles ψ_r and φ_r (i.e., the group velocity to wave vector orientation) as a function of the angle θ that the mirror normal makes with the y axis. The incident parameters were $\psi_i = \varphi_i = 180°$, i.e., the collinear incident beam propagated in the negative y direction (see also Fig. 2). When the mirror normal is parallel to the y axis, the beam reflects backward in the direction $\psi_r = 0$ and *remains collinear* (i.e., $\varphi_r = 0$). As the mirror is gradually inclined, the values of ψ_r and φ_r move apart to different sides relative to the optical axis. [1] For θ in the interval between 15°

[1] The reflected beam parameters can be visualized using Fig. 2, if we draw a straight line corresponding to the orientation of the mirror normal through the end of the incident wave vector $\mathbf{k}_i$ and find the second point where the line intersects the isofrequency curve. This point determines the parameters of the reflected beam. We leave it to the reader to perform such constructions for various values of θ.

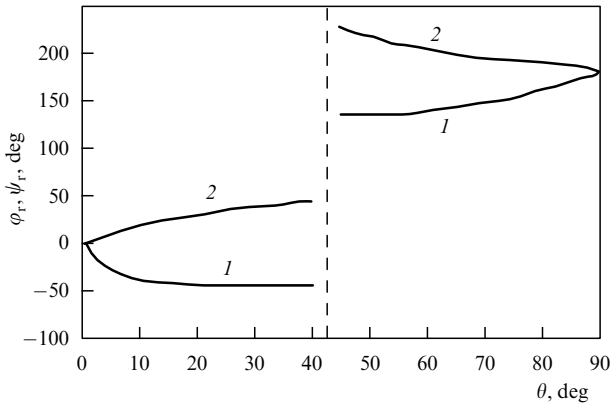

Figure 4. Reflected beam propagation direction ψ_r (curves *1*) and wave vector (front) orientation φ_r (curves *2*) versus mirror orientation θ for a forward wave for $f = 3000$ MHz, $H_0 = 360$ Oe, $4\pi M_0 = 1750$ G, and $s = 10$ μm (all angles are measured from the optical y axis).

and 40°, the beam is reflected at about the same angle, $\psi_r \approx 50°$. This explains why beams in a wide range of incidence angles are reflected in one direction even though the phase front orientation (the angle φ_r) changes smoothly across the reflected beam. For $\theta \approx 43°$, the mirror normal coincides with the isofrequency curve asymptote, making reflection impossible. As the mirror is rotated further, the wave and group velocity vectors turn through 180°, to uniformly converge in the direction of the incident beam. The above results have been confirmed experimentally. We note that knowing ψ_r and θ, it takes straightforward algebra and little effort to calculate the reflection angles χ_r as measured from the mirror normal (see below or, for more details, see Ref. [7]).

Analysis of the reflection from an arbitrarily oriented mirror yields insight into the way a spherical inhomogeneity (for example, just a hole in a film) reflects a plane wave. If the inhomogeneity has its edges smooth and its size much larger than the wavelength, then mirror-like reflection is to occur. We suppose that a plane collinear wave propagates in the negative y direction (i.e., the incident beam corresponds to the point of intersection of curve *2* and the y axis in Fig. 2) and is incident on a circular hole. The part of the circumference that is closest to the point of incidence (and whose middle lies on the y axis) produces reflected beams that correspond to the intersection of the normal with the opposite isofrequency curve (*1* in Fig. 2). This part of the circumference produces backward reflection that converges to a sort of 'knot' on the y axis. The reflection from the remainder of the circumference corresponds to the intersection of the normal with the original isofrequency curve (*2* in Fig. 2) and moves apart in the direction of the incident wave. Analysis shows that part of the backward reflected beams can be focused to a single point by curving the mirror surface in a certain complex way rather than making the boundary circular. It has been estimated theoretically and experimentally [8, 9] that the focal spot can be as small as several fractions of a millimeter. Also, if properly shaped, a strip exciter can be used to focus beams. It is noteworthy that in contrast to the electrodynamics of isotropic media, MSWs are focused by a convex (rather than concave) surface.

We next consider a *backward collinear wave* incident along the z axis on a flat mirror variably oriented with respect to the

optical axis [7]. We directly investigate the dependence of the reflection the angle on the incidence angle $\chi_r(\chi_i)$. The angles χ_i and χ_r were measured from the normal such that if the incident and reflected beams were on different sides of it, the angle χ_r was taken to have the same sign as χ_i; if the two beams were on the same side, χ_r was taken to have the opposite sign to that of χ_i.[2] The orientation of the normal θ and all the remaining angles (the orientation of the group velocities and wave vectors of the incident and reflected beams, ψ_i, ψ_r, φ_i, and φ_r) were measured from the z axis. Clearly, in this picture, the angles of incidence and reflection of the wave, χ_i and χ_r, and the normal orientation (angle θ) are related to the angles ψ_i and ψ_r as

$$\chi_i = \psi_i - \theta + 180^\circ , \tag{15}$$

$$\chi_r = \psi_r - \theta + 360^\circ . \tag{16}$$

The dependence of the reflection angle on the incidence angle $\chi_r(\chi_i)$ is shown in Fig. 5. The direction of the incident wave vector $\mathbf{k}_i$ is opposite to that of the z axis, while the group velocity vector $\mathbf{v}_{gi}$ is along the z axis. The dashed straight line *4* in Fig. 5 shows the reflection pattern for an isotropic medium. As seen from Fig. 5, the backward wave, which is noncollinear in character, undergoes negative reflection from the boundary over the entire range of the incidence angles χ_i (curve *1*) if the incident and reflected waves are described by opposite isofrequency curves (which are analogous to curves *3* and *4* in Fig. 2); if the incident and reflected waves are described by one and the same isofrequency curve (which is analogous to curve *4* in Fig. 2), then negative reflection occurs, observed at incidence angles $|\chi_i| > |\chi_i^{min}|$ (curves *2* and *3*). Therefore, for $|\chi_i| > |\chi_i^{min}|$, a reflected wave may produce two beams, with a negative and a positive χ_r. The value of χ_i^{min} depends on the frequency and on the parameters of the structure (for example, $\chi_i^{min} \approx 37^\circ$ in Fig. 5). The reflection pattern and properties of backward collinear and noncollinear waves, including experimental data, are described in detail in Ref. [7].

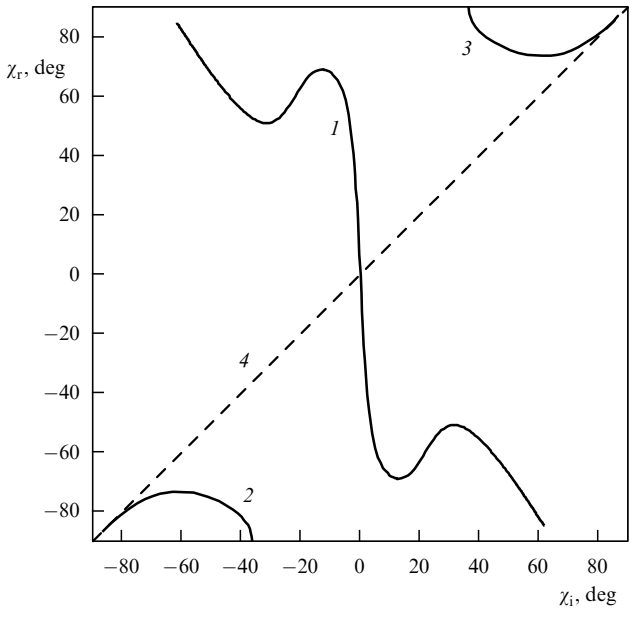

Figure 5. Reflection angle as a function of incidence angle $\chi_r(\chi_i)$ for a backward wave for $f = 2350$ MHz, $H_0 = 367$ Oe, $4\pi M_0 = 1870$ G, $s = 82$ μm: curve *1*, negative reflection; curves *2* and *3*, positive reflection; straight line *4* depicts reflection in isotropic media.

[2] We have to use these conventions for the reflection angle because just this way of measuring the reflection angle is standard and corresponds to the well-known mirror reflection law for isotropic media (the angle of incidence is equal to the angle of reflection).

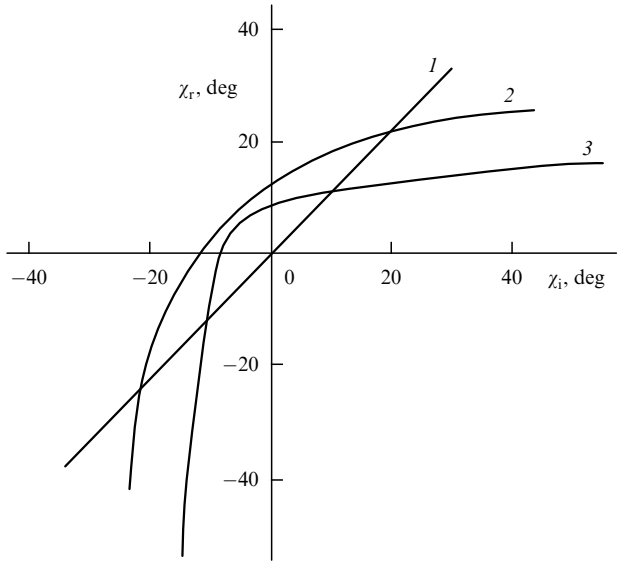

Figure 6. Dependence of the reflection angle on the incidence angle $\chi_r(\chi_i)$ for a forward wave for $f = 3400$ MHz, $H_0 = 437$ Oe, $4\pi M_0 = 1750$ G, and $s = 10$ μm, and various values of the angle θ between the mirror normal and the optical axis: $\theta = 0$ (curve *1*), $\theta = 10^\circ$ (curve *2*), $\theta = 20^\circ$ (curve *3*).

We now consider the dependence of the reflection angle on the incidence angle $\chi_r(\chi_i)$ in the case where the orientation of the flat mirror relative to the optical axis remains unchanged and the incidence angle χ_i is varied by rotating the exciting antenna [3]. We suppose that the antenna excites a *forward wave* described by the isofrequency curve *1* in Fig. 2. Figure 6 shows the calculated dependence of $\chi_r(\chi_i)$ for three different orientations of the mirror. As seen from Fig. 6, if the mirror normal is parallel to the optical axis, then the wave, irrespective of whether it is collinear or noncollinear, is reflected according to Euclid's law (the angle of incidence is equal to the angle of reflection, curve *1*). But if the normal is declined from the optical axis, then, first, the angle of reflection is not equal to the angle of incidence and, second, negative reflection is achieved at small negative values of the incidence angle χ_i (curves *2* and *3* in Fig. 6).

In conclusion, we note that by using noncollinear waves, it is also a simple matter to realize *negative refraction* [10], with both the incident and refracted waves *forward*. Results of the studies above were instrumental in the prototype development of microwave-based analog information processing systems [11].

Acknowledgements. This research was supported in part by the Russian Foundation for Basic Research grant No. 04-02-16460 and the Russian Academy of Sciences Basic Research Program 'The Study of Electrical and Physical Phenomena Related to the Passage of Electromagnetic Energy Flows Through Metamaterials.'

References

1. Damon R W, Eshbach J R *J. Phys. Chem. Solids* **19** 308 (1961)
2. Vashkovsky A V, Shakhnazaryan D G *Radiotekh. Elektron.* **32** 719 (1987)
3. Vashkovskii A V, Zubkov V I *Radiotekh. Elektron.* **48** 149 (2003) [*J. Commun. Technol. Electron* **48** 131 (2003)]
4. Vashkovsky A V, Lokk E G *Elektron. Zh. "Issledovano v Rossii"* **7** 1194 (2004); http://zhurnal.ape.relarn.ru/articles/2004/111.pdf
5. Ivanov V N et al. *Izv. Vyssh. Uchebn. Zaved. Radiofiz.* **32** 764 (1989)
6. Vashkovskii A V, Zubkov V I *Radiotekh. Elektron.* **50** 670 (2005) [*J. Commun. Technol. Electron.* **50** 614 (2005)]
7. Vashkovsky A V, Lokk E G *Usp. Fiz. Nauk* **176** 403 (2006) [*Phys. Usp.* **49** (4) (2006)]
8. Vashkovsky A V et al. *Radiotekh. Elektron.* **31** 837 (1986)
9. Vashkovsky A V et al. *Pis'ma Zh. Tekh. Fiz.* **13** 1067 (1987)
10. Vashkovskiĭ A V, Lokk E G *Usp. Fiz. Nauk* **174** 657 (2004) [*Phys. Usp.* **47** 601 (2004)]
11. Vashkovsky A V et al. *Radiotekh. Elektron.* **35** 2606 (1990)

PACS numbers: **42.25.–p**, 42.70.Qs, 78.20.Ci

DOI: 10.1070/PU2006v049n05ABEH006036

Electromagnetic waves in artificial periodic structures

R A Silin

1. Introduction

The present talk discusses artificial periodic structures for which the propagation of electromagnetic waves is suitably described in terms of the band theory [1], originally developed in solid state physics to study de Broglie waves. Such crystals are of special interest for developing short-wavelength and, in particular, optical-wavelength devices. There is a correspondence between the respective concepts associated with these two kinds of waves (see the Table).

Devices based on such artificial crystals (also known as photonic crystals) include resonators, transmission lines, filters, signal splitters, etc. Underlying their operation are crystal inhomogeneities, which produce local oscillations analogous to impurity levels in a solid, with point inhomogeneities providing a resonator and line inhomogeneities providing a waveguide channel and other radio engineering systems.

Two major spheres of artificial crystal research are the study of wave refraction and reflection at an interface between such crystals and looking for media where waves deviate from their normal behavior. For example, if the group and phase velocities in a medium are opposite, it was shown in [2] that a beam incident from free space is deflected opposite to where it normally should be — a discovery which was followed by a flurry of research on media that are unconventional in the way they reflect and refract waves [3–9]. Most media studied were those transmitting waves in two dimensions, such as two-dimensionally periodic arrays of metallic elements [4–9], ferrite films that carry magnetostatic waves [10, 11], and cholesteric liquid crystals [12]. Plasmas also have unusual reflection and refraction properties [13, 14].

Table. Analogy between de Broglie and electromagnetic waves.

de Broglie waves	Electromagnetic waves
Electron energy $E = \hbar\omega$	Frequency ω
Quasimomentum $\mathbf{p}$	Wave vector $\mathbf{k}$
Electron velocity $\mathbf{v}_c = \mathrm{grad}_{\mathbf{p}}\omega$	Wave group velocity $\mathbf{v}_\Gamma = \mathrm{grad}_{\mathbf{k}}\omega$, equal to the energy transfer velocity
Dispersion characteristic $E(\mathbf{p})$	Dispersion characteristic $\omega(\mathbf{k})$
Energy band	Passband
Forbidden band	Stop band
Isoenergetic surface	Isofrequency
Impurity or surface levels	Local oscillations

One can study beampaths in a medium by considering the electric permittivity tensor ε and the magnetic permeability tensor μ of the medium [13, 14]. But because the calculation of these tensors requires averaging the fields, this approach applies only if the structure period is small compared to the wavelength. A more convenient and user-friendly approach, which is in addition valid for any wavelength, is the method of isofrequencies. Isofrequencies, the surfaces where the wave vector terminates for any wave directions, can be constructed based on the ε and μ tensors and can also be obtained without an averaging procedure.

The analogy between de Broglie waves in crystals and electromagnetic waves in periodic structures led to the discovery of a number of new physical phenomena, to be discussed here.

We consider structures that are periodic in three dimensions. The electromagnetic field in such a structure is expanded in a triple Fourier series of spatial harmonics with wave vectors $\mathbf{k}_{m_1}, \mathbf{k}_{m_2}, \mathbf{k}_{m_3}$ ($-\infty < m_i < \infty$, $i = 1, 2, 3$). Each harmonic corresponds to its own domain of variation (Seitz zone).

The phase velocities of the spatial harmonics are determined by the relation $\mathbf{v}_{m_i} = \omega\mathbf{k}_{m_i}/|\,\mathbf{k}_{m_i}|^2$ and are different, whereas the group velocities $\mathbf{v}_\Gamma = \mathrm{grad}_{\mathbf{k}}\omega$ are all equal. The group velocity determines the direction of the flow of energy (or the beam, or information) and is directed along the normal to the isofrequency and toward higher frequencies.

Knowing the phase velocities, wave vectors, and harmonic amplitudes of electromagnetic waves is important because these quantities determine the direction and intensity of diffraction peaks (e.g., in diffraction and antenna gratings). This knowledge is also essential in studying the interaction of electrons with a wave (the Vavilov–Cherenkov effect). In a one-dimensionally periodic medium, this interaction is strongest when the phase velocity $v = \omega/k$ is close to the electron velocity ($v_e \approx \omega/k$), i.e., $kv_e = \omega$. The extension of this relation to two- and three-dimensional systems is given by the Vavilov–Cherenkov condition $\mathbf{k}\mathbf{v}_e = \omega$, known in high-frequency technologies as the condition for electron–wave *synchronism* and used in developing electronic devices (traveling wave tubes, backward wave tubes, etc.).

2. Wave vector construction using isofrequencies

We generally distinguish between *forward* and *backward* waves. The term forward refers to a wave in which the angle θ between the phase and group velocities does not exceed $\pi/2$ ($|\theta| < \pi/2$). In the case where $\pi/2 < |\theta| \leqslant \pi$, the wave is said to be backward.

Figure 1 depicts the cubic elementary cells of two artificial media and shows plots, in the k_x, k_y plane, of their respective isofrequencies for the zero zone in the second transmission band. The numbers labeling the curves are proportional to the frequencies and represent the values of a/λ, where a is the size

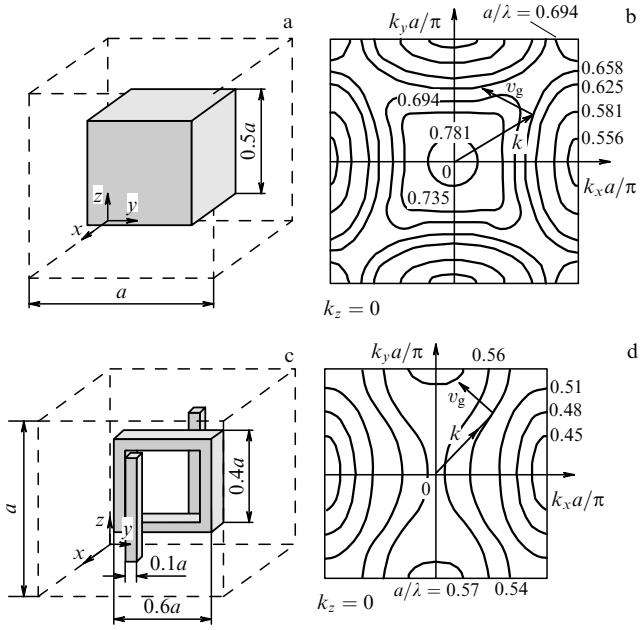

Figure 1. Examples of elementary cells of three-dimensional periodic structures and their isofrequencies constructed in coordinates k_x, k_y in the zero zone and calculated in the second passband.

of the cell and λ is the wavelength in free space. Also shown are the wave vectors and group velocity directions (bold and thin arrows, respectively).

We use isofrequencies ($a/\lambda = \text{const}$) to consider the refraction of a wave at the interface of two isotropic media and the path of beams ($\mathbf{v}_b$) for waves that have passed through a parallel-plane plate. In Fig. 2, panels a, b, and e correspond to a forward wave, and c, d, and f to a backward wave in a refracting medium. Shown dashed in Fig. 2 and all the following figures are the projections of the vectors $\mathbf{k}$ on the abscissa. We note that the energy of the refracted wave is transferred from the interface between the two media and that the projections on the interface of the incident ($\mathbf{k}_{inc}$), reflected ($\mathbf{k}_{reflec}$), and refracted ($\mathbf{k}_{refrac}$) waves are equal (Figs 2a – d).

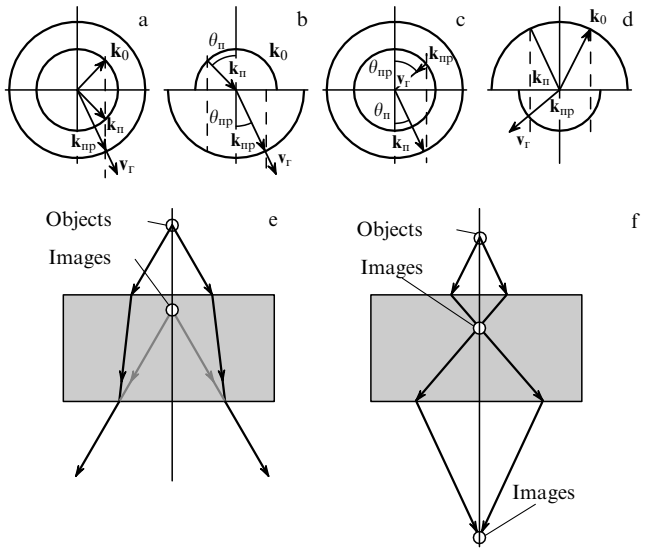

Figure 2. Wave vectors $\mathbf{k}$ and beams $\mathbf{v}_b$, and objects and images in the cases where a wave passes through the interface between two media (a, b, c, d) and through a plate (e, f). Diagrams a, b, e: a forward wave traveling in a refractive medium and a plate; diagrams c, d, f: the same for a backward wave. Constructions in diagrams a and c are rigorous but difficult to grasp; those in b and d are easy to grasp but not rigorous.

Two different vectors $\mathbf{k}_{refrac}$ may have equal projections on the interface in a refractive medium. One of the vectors (Fig. 2a) is directed from the interface downward and corresponds to a forward wave, whereas the other (Fig. 2c) is directed upward and corresponds to a backward wave. Of these two, the one that corresponds to the group velocity (beam) directed from the interface belongs to the refracted wave (compare Figs 2a, b and Fig. 2c, d). For each case in Fig. 2, two constructions are made. One of them, in which the vectors are always directed from the origin (Figs 2a, c), is rigorous and always yields the directions of all the vectors in a unique way. The rigorous construction is rather involved, however. In an approach used more frequently (Figs 2b, d), the wave vectors of the incident wave are depicted in the upper half-plane and those of the refracted wave in the lower half-plane. This construction, however, although easier to grasp, sometimes leaves one uncertain as to the direction of the beam.

Figures 2e, f demonstrate the course of beams for the forward (Fig. 2e) and backward (Fig. 2f) waves in a plate and demonstrate the images of objects in these plates. In the case of a forward wave, the object and its image are on the same side of the plate. For a backward wave, two images are possible, one of them lying on the other side of the plate.

Backward waves and their associated propagation media and refraction laws have been known for a long time now [3, 4, 8]. In 1940 – 1966, these waves were widely used in backward wave tubes and antennas. Pafomov [1] showed [13] that backward waves are possible in an isotropic medium with both a negative electric permittivity ε and a negative magnetic permeability μ. Such a phenomenon can be observed in plasma [13, 14]. It was only in 2000, i.e., about forty years after Refs [3, 4, 8], that Ref. [16] suggested a medium — a periodic array of metal rods and rings — that can support a backward wave in one dimension and in the second passband only. The isofrequencies of this structure are similar to those shown in Fig. 1d.

The discussion above is limited to isotropic media, in which isofrequencies form spherical or circular shapes centered at the origin. In reality, however, propagation media only behave isotropically in a certain limited frequency band (Fig. 1b). The construction of wave vectors and beams, i.e., group velocities, for isofrequencies of different forms is illustrated in Fig. 3. There are two diagrams corresponding to each shape: for the passage of waves and beams through the interface between two media and for the passage through a plate; in the former case, free-space isofrequencies (origin-centered semicircles) and medium isofrequencies are shown in the upper and lower half-planes, respectively. Figure 3a corresponds to media assumed to support a forward wave.

The situation in Fig 3a, with the interface parallel to the $\mathbf{k}_x$ axis, may occur for the isofrequency $a/\lambda = 0.57$ shown in Fig. 1d. An unusual feature is here that the object and its image lie on different sides of the plate even though the wave

[1] Although the proof of the existence of backward waves in $\varepsilon < 0$, $\mu < 0$ media is often mistakenly credited to V G Veselago [15], it is in fact V E Pafomov who first did it.

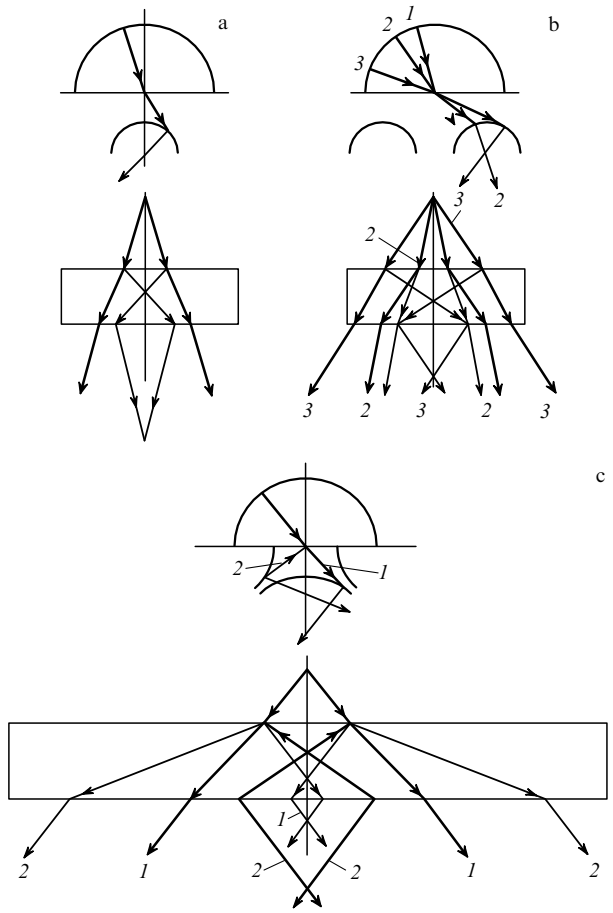

Figure 3. Wave vectors (bold arrows) and beams (thin arrows) corresponding to wave passage from free space through the interface between two media and through parallel-plane plates of materials with different isofrequency shapes.

is forward. The opposite should be observed when the corresponding isofrequency ($a/\lambda = 0.556-0.658$ in Fig 1b, $a/\lambda = 0.45-0.56$ in Fig. 1d) is that of a backward wave. In this case, the beam is deflected from the normal to the same side as in a dielectric, and the object and its image lie on the same side of the lower boundary of the plate (as in Fig. 2e). The situation shown in Fig. 3b is possible for isofrequencies $a/\lambda = 0.694$ (Fig. 1b) when the interface normal is parallel to either the $\mathbf{k}_x$ or $\mathbf{k}_y$ axis. At small incidence angles (wave vector *1*), the wave does not penetrate into the artificial medium because no isofrequencies at which the wave vector can terminate exist in this medium. As the incidence angle increases, the wave starts to penetrate the medium, and the refraction angle first increases and then changes sign.

We next consider Fig. 3b, which corresponds to the isofrequencies shown in Fig. 1b ($a/\lambda = 0.658$). In a refractive medium, there are two wave vectors with equal projections on the interface, and therefore two refracted beams may correspond to one beam in the incidence wave (*birefrigence*), with the result that the object turns out to have two images (beams *1* and *2* converge at different points). Importantly, the polarization of either beam remains the same here, in contrast to birefrigence in conventional optics.

Of greater interest are waves in ferrite films that are placed between metallic planes and subjected to a magnetic field (Fig. 4). In such systems, there exist isofrequencies that are intersected only once by a straight line perpendicular to the

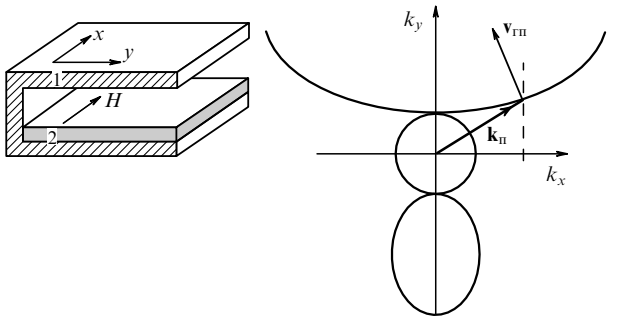

Figure 4. Isofrequencies of a ferrite film on a dielectric substrate, and incident vectors $\mathbf{k}_п$ and $\mathbf{v}_{гп}$ for the case where no reflected and no refracted wave are present.

interface, suggesting that something seemingly unreasonable may happen: an incident wave from which neither a refracted wave nor a reflected wave arises. This effect was predicted in Ref. [10] and observed experimentally in Ref. [11]. (We note parenthetically that the energy that comes to the interface is carried away by an edge wave).

3. Backward-wave supporting media

Two-dimensionally periodic lattices capable of supporting backward waves were described back in 1959 in Refs [3, 4], the former of which proposed a structure where, unlike those in today's publications, backward waves exist in the first passband.

According to Rayleigh, who proved the possibility of backward waves in 1877, the phase and group velocities of such a wave are related by

$$n_г = n - \lambda \frac{\mathrm{d}n}{\mathrm{d}\lambda},$$

where $n = c/v$ and $n_г = v/v_г$ are the phase and group velocity retardation factors. At sufficiently high dispersion $\mathrm{d}n/\mathrm{d}\lambda > 0$, the quantities $n_г$ and n are opposite in sign, thus giving rise to a backward wave.

Structures in which backward waves are allowed to run in only one or two dimensions have been known since 1904 (Lamb) and have been widely used in electronic and antenna engineering, starting from 1952. Backward waves also exist in cholesteric liquid crystals [12], partially dielectric waveguides, and many other systems.

Backward waves of the zero spatial harmonic in the fundamental (i.e., longest-wavelength) passband have been detected in one- and two-dimensionally periodic structures [3–8], but no three-dimensionally periodic structures with such properties are known. A second-band backward wave is relatively easy to obtain (see Ref. [5] and Fig. 1).

4. Conclusion

Artificial crystals are of particular interest for application in and around the optical part of the spectrum. Using such crystals allows developing integrated circuits, electronic instruments, and devices with unusual optical properties. In particular, not only a parallel-plane lens but also a plate can be given a property of being opaque to a normally incident wave while transmitting an obliquely incident one. Another possibility is a plate that exhibits birefrigence the amount of

which depends on the frequency and the angle of incidence rather than the polarization of the beam. For a ferrite film in a magnetic film, a wave incident on the edge of the film neither is reflected from nor passes through the film. All these results are readily obtained using the isofrequency concept.

In conclusion, we note that the existence of backward waves in media with $\varepsilon < 0$ and $\mu < 0$ was first proved by V E Pafomov [13], not by V G Veselago in Ref. [15]. Backward waves and their unusual refraction properties in artificial crystal were first discussed by the present author [3, 4], not by Smith et al. in Ref. [16].

References

1. Seitz F *The Modern Theory of Solids* (New York: McGraw-Hill Book Co., 1940) [Translated into Russian (Moscow – Leningrad: GITTL, 1949)]
2. Mandelstam L I *Polnoe Sobranie Trudov* (Comple Works) Vol. 5 (Moscow: Izd. AN SSSR, 1950) p. 461
3. Silin R A *Vopr. Radioelektron. Ser. 1. Elektronika* (4) 3 (1959)
4. Silin R A, Sazonov V P *Zamedlyayushchie Sistemy* (Retarding Systems) (Moscow: Sov. Radio, 1966)
5. Silin R A, Chepurnykh I P *Radiotekh. Elektron.* **46** 1212 (2001) [*J. Commun. Technol. Electron.* **46** 1121 (2001)]
6. Silin R A *Neobychnye Zakony Prelomleniya i Otrazheniya* (Unusual Laws of Refraction and Reflection) (Moscow: Fazis, 1999)
7. Silin R A *Radiotekh. Elektron.* **5** 688 (1960)
8. Silin R A *Izv. Vyssh. Uchebn. Zaved. Radiofiz.* **15** 809 (1972)
9. Silin R A *Opt. Spektrosk.* **44** 189 (1978) [*Opt. Spectrosc.* **44** 109 (1978)]
10. Demchenko N P, Nefedov I S, Silin R A, in *Vzaimodeistvie Elektromagnitnykh Voln s Poluprovodnikami i Poluprovodnikovo-dielektricheskimi Strukturami i Problemy Sozdaniya Integral'nykh KVCh Skhem* (Interaction of Electromagnetic Waves with Semiconductors and Semiconductor-Dielectric Structures and Problems of Development of High-Frequency Microwave Circuits) Pt. 2 (Saratov: Izd. Saratovskogo Gos. Univ., 1985) p. 94
11. Vashkovsky A V, Stal'makhov A V, Shakhnazaryan D G *Izv. Vyssh. Uchebn. Zaved. Fiz.* **31** (11) 67 (1988) [*Sov. Phys. J.* **31** 908 (1988)]
12. Byrdin V M *Opt. Spektrosk.* **54** 456 (1983) [*Opt. Spectrosc.* **54** 268 (1983)]
13. Pafomov V E *Zh. Eksp. Teor. Fiz.* **36** 1853 (1959) [*Sov. Phys. JETP* **9** 1321 (1959)]
14. Agranovich V M, Ginzburg V L *Kristallooptika s Uchetom Prostranstvennoi Dispersii i Teoriya Eksitonov* (Crystal Optics with Spatial Dispersion, and Excitons) (Moscow: Nauka, 1965) [Translated into English (Berlin: Springer-Verlag, 1984)]
15. Veselago V G *Usp. Fiz. Nauk* **92** 517 (1967) [*Sov. Phys. Usp.* **10** 509 (1967)]
16. Smith D R et al. *Phys. Rev. Lett.* **84** 4184 (2000)